A Raman and FIR spectroscopic study of the solid solution $(N(CH_3)_4)_2ZnCl_{4-x}Br_x$

1991 J. Phys.: Condens. Matter 3 8113

(http://iopscience.iop.org/0953-8984/3/41/010)

J. Phys.: Condens. Matter 3 (1991) 8113–8126. Printed in the UK

A Raman and FIR spectroscopic study of the solid solution $(N(CH_3)_4)_2ZnCl_{4-x}Br_x$

P H M van Loosdrecht† and A Janner‡

† Research Institute of Materials, University of Nijmegen, Toernooiveld, 6525 ED Nijmegen, The Netherlands

‡ Institute of Theoretical Physics, University of Nijmegen, Toernooiveld, 6525 ED Nijmegen, The Netherlands

Received 19 March 1991, in final form 31 May 1991

Abstract. Polarized Raman and far-infrared spectra (10–350 cm^{-1}) of the solid solution $(N(CH_3)_4)_2ZnCl_{4-x}Br_x$ are presented for several compositions ($x = 0$, 1, 2, 2.9 and 4) in the high- (300 K) and low- (60 K) temperature phases of the crystals. Apart from the internal modes of the $ZnCl_4^{2-}$ and $ZnBr_4^{2-}$ ions, several new active internal modes are found in the spectra, originating from the mixed $(ZnCl_{4-n}Br_n)^{2-}$ ions ($n = 1$, 2, 3 and 4). The spectra are in fair agreement with a simple 'free' ion model for the vibrational modes of the $(ZnCl_{4-n}Br_n)^{2-}$ ions. From the intensities of the tetrahedral ν_1 modes, the relative concentrations of the various $(ZnCl_{4-n}Br_n)^{2-}$ ions in the crystals are estimated. Using these relative concentrations the value of x in the crystals is calculated, and found to be in good agreement with the stoichiometries of the crystal growth solutions. A pronounced low-frequency mode is observed in the spectra which scales with the average moment of inertia of the $(ZnCl_{4-n}Br_n)^{2-}$ ions, and is therefore assigned to a librational mode of these ions.

1. Introduction

The solid solution $(N(CH_3)_4)_2ZnCl_{4-x}Br_x$ belongs to the A_2BX_4 family of dielectrics, having in general an orthorhombic (β-K_2SeO_4) high-temperature phase. At lower temperature, different sequences of modulated phases are found for the members of this family, among which an incommensurate one is often found. The many common structural features among the members leads to the assumption that the modulation in this family has a common origin (Janssen 1986, Godefroy 1987). In fact, for many members the phases (both commensurate and incommensurate) can be described to a very good approximation as different three-dimensional intersections of a four-dimensional structure, with a single superspace group symmetry (the prototype symmetry group).

A few years ago, Colla *et al* (1984) determined the x–T phase diagram of the solid solution $(N(CH_3)_4)_2ZnCl_{4-x}Br_x$ (tetramethylammonium-tetra(chloro,bromo)zincate, hereafter denoted by TZCB). They found a rich variety of phases and phase transitions. The phase transitions in this system result mainly from modulated rotations $(\theta_x, 0, \theta_z)$ and translations $(0, t_y, 0)$ of the $N(CH_3)_4^+$ and of the $(ZnCl_{4-n}Br_n)^{2-}$ (hereafter denoted by ZCB_n^{2-}) tetrahedra. At high temperature ($T > 293$ K) the phase has space group symmetry *Pnma* for all compositions. At lower temperature the pure

0953-8984/91/418113+14$03.50

chloride compound exhibits phase transitions (Sawada *et al* 1978) to respectively an incommensurate phase, an orthorhombic, two monoclinic and finally an orthorhombic phase again. The pure bromide compound, however, only exhibits one phase transition to a monoclinic low-temperature phase (Gesi 1982, Trouelan *et al* 1985). The modulated incommensurate phase present in the $x = 0$ compound disappears at $x \approx 3$. Near $x \approx 3$, the wavevector of the modulation continuously changes from an incommensurate to a commensurate value. Indeed, this is exceptional, as usually one observes a discontinuous jump of the order of 10^{-2} to the rational value in the modulation parameter. The continuity of the modulation parameter is interesting in view of a possible additional electromagnetic propagation mode in incommensurate structures with a nearly commensurate modulation, as predicted by van Beest (1986).

The purpose of the present paper is to obtain a better insight into the basic vibrational properties of TZCB. In order to study these properties we have performed Raman and far-infrared (FIR) spectroscopic experiments on several solid solutions in their high- and low-temperature phases. An extensive Raman investigation of the pure Cl compound has already been performed by Meekes *et al* (1988). We have concentrated our attention on the region of ZCB_n^{2-} vibrational modes, not only because of their relation to the phase transitions in this material, but also in order to obtain a better understanding of the distribution of Cl and Br in this system. The Cl,Br distribution is expected to influence both the selection rules and the intensities in Raman and FIR experiments, as will be shown in sections 3 and 4.

This paper is organized as follows. In section 2 the experiments are described and the resulting spectra are presented. The activity of the internal ZCB_n^{2-} modes is discussed in terms of the free tetrahedral ion symmetry modes in section 3. In section 4 the spectra presented in section 2 are discussed. Finally, in section 5 some conclusions are given.

2. Experimental procedure

The crystals used in the experiments are grown from a seed in an aqueous solution of a stoichiometric mixture of $(N(CH_3)_4)Y$ and ZnY_2 (Y = Cl, Br) by a slow convection method (Arend *et al* 1986). In this way, optically transparent crystals (~ 1 cm^3) were obtained from a solution with a known bromide concentration (x). The actual Br concentration is expected to be somewhat higher than this value. The crystals are oriented using their rich morphology (Dam and Janner 1986, Vogels 1990). The unit-cell dimensions for a crystal with $x = 2.9$ are determined by x-ray diffraction to be $a = 12.49$ Å, $b = 9.24$ Å and $c = 15.90$ Å, which is consistent with the results of Arend *et al* (1986).

For the polarized Raman experiments, the crystals are cut and polished to platelets (dimension $\sim 2 \times 3$ mm^2, 0.5–1 mm thick). The platelets are mounted in an Oxford cryostat (temperature stabilization better than 1 K). The Raman spectra are recorded in a standard way (90° geometry) using the 514.5 nm line of an Ar^+ laser (unfocused, power < 250 mW) as the exciting source.

The TZCB crystals have a strong absorption in the FIR region, making it very difficult to measure the absorption directly on single crystals. In order to be able to obtain FIR absorption spectra, we have therefore powdered the crystals and embedded them in a polyethylene platelet (~ 0.35 mm thick). In this way, samples are obtained with a known low molar concentration of the crystal ($\sim 5\%$). The unpolarized

FIR transmission spectra were measured at room temperature using a Bruker FT-IR spectrometer.

2.1. *FIR experiments*

FIR transmission spectra of the powdered samples embedded in a polyethylene matrix were measured relative to the transmission of pure polyethylene. Some typical spectra at room temperature for $x = 0$, 1, 2.9 and 4 are shown in figure 1. As x increases some modes shift in frequency and new modes appear in the spectra, although the modes of the mixed tetrahedra are not resolved in this case. The structure at 456 cm^{-1} present in all spectra is due to the tetrahedral ν_4 symmetry modes of the $N(CH_3)_4^+$ ions (Edsall 1937). The ν_3 and ν_4 modes of $ZnCl_4^{2-}$ and $ZnBr_4^{2-}$ are clearly visible as broad absorption lines in the spectra.

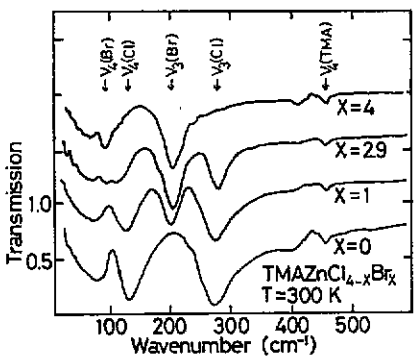

Figure 1. Room temperature FIR transmission spectra of powdered TZCB crystals ($x = 0$, 1, 2.9 and 4) embedded in a polyethylene matrix. A pure polyethylene sample has been taken as a reference.

2.2. *Raman experiments*

Polarized Raman spectra are measured for $x = 0$, 1, 2, 2.9 and 4 in the high- and low-temperature phases. As already mentioned, we focused on the frequency range of the internal ZCB_n^{2-} modes $\nu_1, \ldots, \nu_4$ (10–350 cm^{-1}) (Morris *et al* 1963). There are two regions of interest in the spectra. The first one (10–150 cm^{-1}) contains the external modes and the ν_2 and ν_4 internal ZCB_n^{2-} modes, whereas the second one (150–350 cm^{-1}) contains the ν_1 and ν_3 internal modes of the ZCB_n^{2-} tetrahedra. The internal modes of the $N(CH_3)_4^+$ ions lie at higher frequencies (Edsall 1937). The results of the Raman experiments can be found in figure 2(*a*) ($T = 300$ K) and 2(*b*) ($T \approx 60$ K). Raman spectra of different crystals are generally difficult to compare quantitatively due to the variations of for instance the optical quality of the samples. In order to get a better quantitative comparison of the spectra, we have therefore normalized the spectra of the crystals with a different composition in figure 2(*a*) and 2(*b*) with respect to the integrated intensity of the 150–350 cm^{-1} region in A_g geometry of the same crystal, thereby assuming that the scattering efficiency of the ZCB_n^{2-} tetrahedra is approximately the same for all n.

In the monoclinic low-temperature phases, domains differing in monoclinic angle, and a rotation of the indicatrix around the unique axis are observed under a polarization microscope. Due to the rotation of the indicatrix, light polarized along one

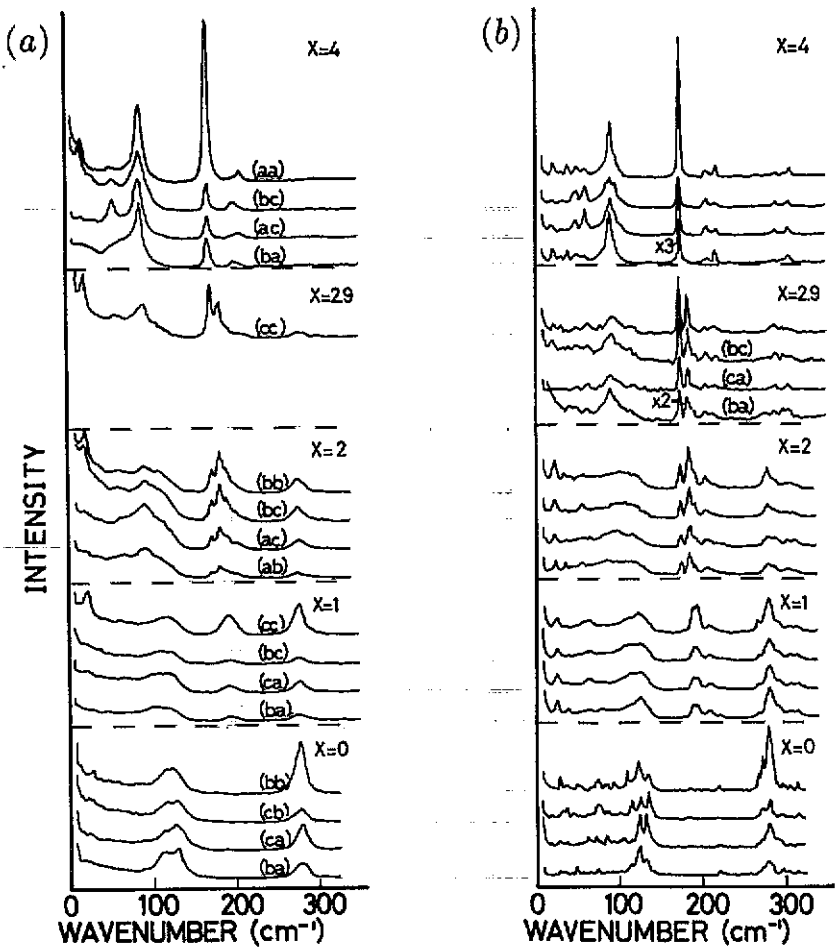

Figure 2. (*a*) Polarized Raman spectra at $T = 300$ K of the solid solution TZCB for $x = 0$, 1, 2, 2.9 and 4. Clearly new modes appear in the spectra of the mixed crystals resulting from the internal modes of the mixed ZCB_n^{2-} ions. The scattering geometry is indicated for each curve ((a, b) means incoming polarization along a, polarization of the scattered light along b). The corresponding irreducible representations of the point group can be found in table 2. (*b*) Polarized Raman spectra at $T \approx 60$ K of the solid solution TZCB for $x = 0$, 1, 2, 2.9 and 4. The scattering geometries are the same as in (*a*). The corresponding irreducible representations can be found in table 3.

of the two non-unique axes becomes elliptical, resulting in a mixing of the scattering polarizations.

In the spectra of the mixed crystals new modes appear due to the mixed character of the ZCB_n^{2-} anions. Also some modes shift in frequency as function of the composition and/or the temperature. This is illustrated by the measurement of the lattice mode at ~ 24 cm^{-1} for several temperatures (figure 3(*a*)) and by the comparison of the frequencies of this mode for different mixing ratios (figure 4).

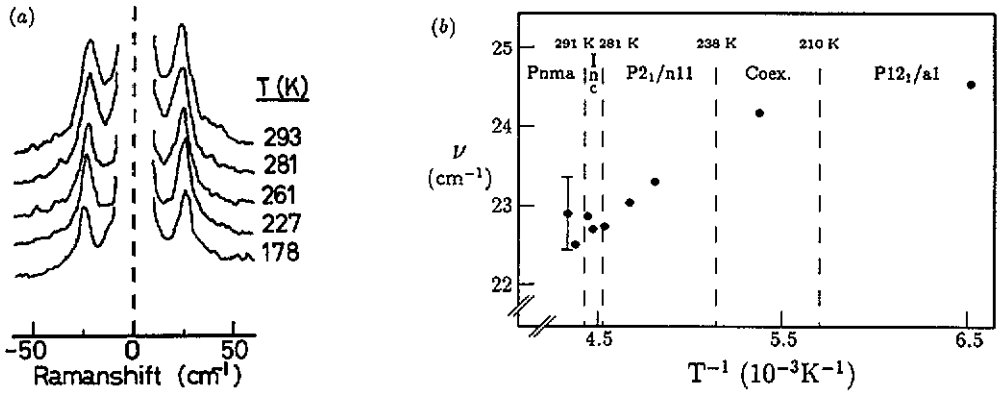

Figure 3. (*a*) Stokes and anti-Stokes A_g Raman spectra of the ~ 24 cm^{-1} mode and the quasi-elastic scattering in TZCB for $x = 1$ at various temperatures. (*b*) Temperature dependence of the ~ 24 cm^{-1} mode in an $x = 1$ crystal. The mode is insensitive to the phase transition to the incommensurate phase. A hardening of this mode is observed after the phase transition to the monoclinic $P2_1n11$ phase.

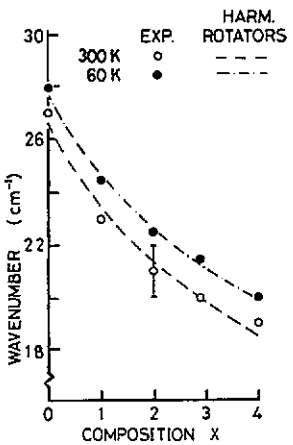

Figure 4. Composition dependence of the ~ 24 cm^{-1} mode at $T = 300$ K (●) and at $T = 60$ K (○). The mode scales with the average mass of the outer atoms of the heavy ZCB_n^{2-} tetrahedra. This is shown by the broken curves which are fits of the data for a chain of classical harmonic rotators, with frequency $\nu^2 \sim I^{-1}$ (I = moment of inertia).

3. Raman and IR activity of the $(ZnCl_{4-n}Br_n^{2-})$ modes

Before we turn to the actual activity of the ZCB_n^{2-} modes, we will first make some remarks on the structure of the TZCB crystals. At room temperature the structure of TZCB is isomorphic for all x. The space group is *Pnma* ($Z = 4$). The unit-cell dimensions change continuously from $a = 12.268$ Å, $b = 8.946$ Å and $c = 15.515$ Å for $x = 0$ to $a = 12.681$ Å, $b = 8.238$ Å and $c = 16.025$ Å for $x = 4$ (Arend *et al* 1986). The structure is built up from more or less rigid $N(CH_3)_4^+$ and ZCB_n^{2-} tetrahedra positioned at $(x, \frac{1}{2}, z)$ with site symmetry C_s in the pure crystals. On lowering the temperature, the TZCB crystals undergo several structural phase transitions, resulting

mainly in rotations $(\theta_x, 0, \theta_z)$ and translations $(0, t_y, 0)$ of the tetrahedra. Due to the rotations, the site symmetry of the tetrahedra changes from C_s to C_1 (the mirror plane m_y is lost). The low-temperature phases have been determined for the $x = 0$ (Sawada 1978), $x = 2.2$ (Colla 1987) and $x = 4$ (Trouelan 1985) compounds. The space groups of the $x = 0$ and $x = 4$ compounds are respectively orthorhombic $P2_12_12_1$ ($Z = 12$, $T < 161$ K) and monoclinic $P112_1/a$ ($Z = 4$, $T < 287$ K). For the mixed crystals we assume that the low-temperature structures are those found in the phase diagram by Colla *et al* (1984), that is $P12_1/a1$ ($Z = 8$, $T < 210$ K) for $x = 1$ and $x = 2$ crystals, and $P112_1/a$ ($Z = 4$, $T < 273$ K) for $x = 2.9$ crystals.

3.1. Free ion approximation

Since we consider the structure as being built up from rigid tetrahedra, we can discriminate between the internal tetrahedra modes and the external vibration modes (including the vibrational and librational modes of the rigid tetrahedra). The validity of this assumption will be considered later, when we discuss the experimental results. We only consider phonons with wavevector $k = 0$.

Here we restrict ourselves to a discussion of the internal ZCB_n^{2-} modes. We first consider the 'free' ZCB_n^{2-} anions, neglecting the crystal field and the coupling between the ions. The point group of the ZCB_n^{2-} anions depends on the value of n. For $n = 0$ and $n = 4$ ions the point group is T_d, for $n = 1$ and $n = 3$ ions C_{3v} and for the $n = 2$ ions C_{2v}. In figure 5 the correlation diagram of the vibrational modes for these various point groups is given. Since C_{2v} is not a subgroup of C_{3v}, the correlations can not be determined by a direct subduction. Instead, the correlation is found by a projection of the C_{3v} modes onto the C_{2v} modes.

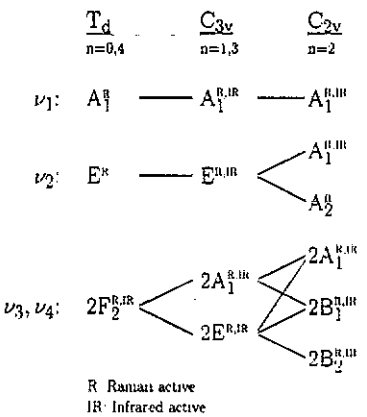

Figure 5. Correlation diagram of the symmetry modes of the free ZCB_n^{2-} tetrahedra in different compositions. (T_d: $n = 0$ or 4, C_{3v}: $n = 1$ or 3 and C_{2v}: $n = 2$).

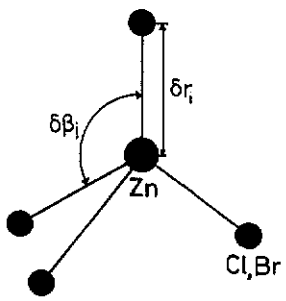

Figure 6. Zn–Y stretching (δr_i) and Y–Zn–Y bending ($\delta\beta_j$) coordinates in a tetrahedral ZnY_4 ion, where Y stands for Cl, Br.

Figure 5 shows that the degenerate modes in the pure ions split up in the mixed cases. One can gain some more insight into this splitting by considering a simple valence-bond model for the ions, which we discuss briefly now. In this model we

consider the change of mass upon substituting a Cl atom by a Br atom. The valence bond potential is taken to be

$$V = \sum_{i=1}^{4} \lambda_i (\delta r_i)^2 + \sum_{j=1}^{6} \mu_j (\delta \beta_j)^2$$

where δr_j and $\delta \beta_j$ are respectively the Zn–Y stretching and Y–Zn–Y bending co-ordinates (see figure 6). The force constants λ_i, μ_j are determined from the ν_1 and ν_2 ZCB_n^{2-} mode frequencies in the pure compounds using (for T_d symmetry)

$$\nu_1^2 = \lambda/m \qquad \text{(Zn–Cl, Zn–Br stretching)}$$
$$\nu_2^2 = \mu/3m \qquad \text{(Cl–Zn–Cl, Br–Zn–Br bending)}$$

with m the mass of either a Cl, or a Br atom. For the Cl–Zn–Br bending force constant a linear interpolation between the two pure cases is used. The resulting force constants are shown in table 1. The model uses only two (T_d symmetry) or four (C_{2v} and C_{3v} symmetry) independent force constants, whereas the actual problem has more (4 for T_d, 6 for C_{3v} and 9 for C_{2v} symmetry). This leads for instance to a higher frequency for the ν_3 modes of the ions. Despite the restrictions of the model, we think that it gives a clear qualitative picture of the vibrational properties of the heavy tetrahedra. The frequencies of the symmetry modes of the various ions are determined by solving the dynamical matrix of the model. The results of this calculation are shown in figure 7. Three groups of modes are found for the tetrahedra, based on the symmetry modes $\nu_1, \ldots, \nu_4$ of the pure ions. The ν_3 group at 310–390 cm^{-1}, the ν_1 group at 180–280 cm^{-1} and the ν_2,ν_4 group at 80–130 cm^{-1}. In all groups, the frequency generally decreases as n is increased, which is expected because of the greater mass of the Br atoms. The splitting of the modes expected from group theory is clearly observed in the model (figure 7). The ν_3 modes seem to give the best opportunity to measure it because of the relatively large splitting of these modes, whereas the ν_2 and ν_4 modes are probably too closely spaced. If TZCB is a true solid solution, then all the different anions ZCB_n^{2-} will in general be present in the crystals, and all the modes presented in figure 7 are expected to be observable as internal modes in Raman and FIR experiments. We return to this model in the next section, where the results of the Raman and FIR experiments are discussed.

Table 1. Force constants used in the valence-bond model, calculated from the frequencies of the ν_1 and ν_2 modes in the pure compounds.

Zn-Cl stretching (ν_1=278cm^{-1})	λ=160 N/m
Zn-Br stretching (ν_1=170cm^{-1})	λ=136 N/m
Cl-Zn-Cl bending (ν_2=116cm^{-1})	μ=9 N/m
Br-Zn-Br bending (ν_2=56cm^{-1})	μ=5 N/m
Cl-Zn-Br bending	μ=7 N/m

3.2. Tetrahedral modes in the crystals

We now turn to the activity of the internal ZCB_n^{2-} modes in the crystals. In table 2 the activities of these modes in the high-temperature *Pnma* phase are given. This

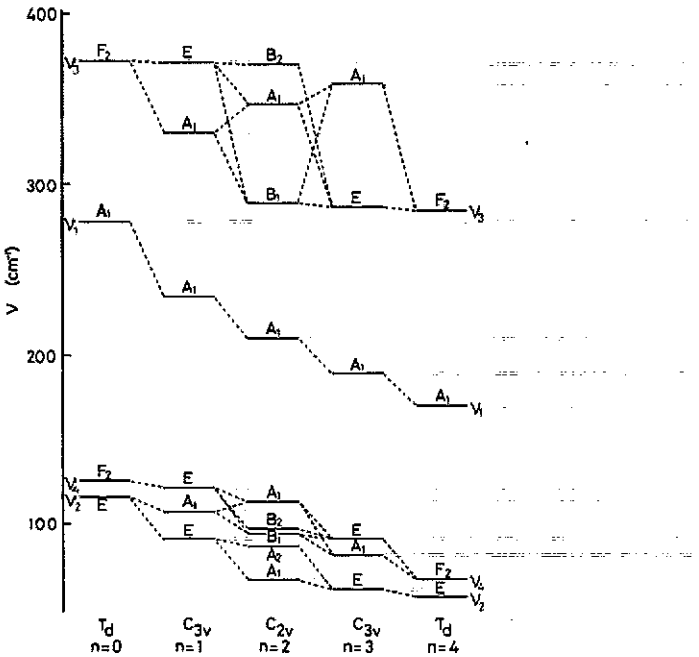

Figure 7. Vibrational energy levels calculated from a valence bond potential model for the various ZCB_n^{2-} anions. The force constants used, and the characteristic features of this model are discussed in section 3.

table is based on the site symmetry C_s for the ZCB_n^{2-} ions. In the mixed crystals however, this mirror symmetry may be lost. This is, in particular, the case when the two atoms which are outside the mirror plane m_y are of a different kind. In that case the site symmetry is C_1, and the modes will be active in all geometries (in both Raman and FIR experiments). If the substitution of Cl by Br is totally disordered, the site symmetry will also be C_1.

Table 2. Raman and infrared activity of the internal ZCB_n^{2-} modes in the high-temperature *Pnma* phase of the TZCB crystals. The site symmetry of the ions is C_s.

Pnma (Z=4)			site symmetry C_s	
D_{2h}	ν_1	ν_2	$\nu_3+\nu_4$	activity
A_g	1	1	4	(a,a),(b,b),(c,c)
B_{1g}	0	1	2	(b,c)
B_{2g}	1	1	4	(a,c)
B_{3g}	0	1	2	(a,b)
A_u	0	1	2	-
B_{1u}	1	1	4	a
B_{2u}	0	1	2	b
B_{3u}	1	1	4	c

The above differences in site symmetry, and thus in selection rules, gives a means to determine whether there is some kind of ordering, leaving the mirror m_y intact. This is for instance the case if the substitution of Cl by Br preferentially takes place

on the Y site of the tetrahedra with the smallest thermal motions (Colla *et al* 1987), with Zn–Y in the mirror plane, and the bond along *a*.

At low temperatures the site symmetry of the tetrahedra is always C_1, leading to an activity of all modes in all geometries. However, detectable in the spectra is the number of different frequencies of a given mode, due to the presence of a different number of tetrahedra in the primitive cell of the compounds, and the mixed character of the tetrahedra. The activity of the ZCB_n^{2-} modes are given in table 3(*a*) for $x = 0$, in table 3(*b*) for $x = 1$ and $x = 2$, and in table 3(*c*) for the $x = 2.9$ and $x = 4$ compounds.

Table 3. Raman and infrared activity of the internal ZCB_n^{2-} modes in the low-temperature phases of the various TZCB crystals. The site symmetry is C_1 in all cases. (*a*) $x = 0$ crystals, space group $P2_12_12_1$ ($Z = 12$). (*b*) $x = 4$ and $x = 2.9$ crystals, space group $P112_1/a$ ($Z = 4$). (*c*) $x = 1$ and $x = 2$ crystals, space group $P12_1/a1$ ($Z = 8$).

a. $P2_12_12_1$ (Z=12) site symmetry C_1					b. $P112_1/a$ (Z=4) site symmetry C_1				
D_2	ν_1	ν_2	$\nu_3+\nu_4$	activity	C_{2h}	ν_1	ν_2	$\nu_3+\nu_4$	activity
A	3	6	18	(a,a),(b,b),(c,c)	A_g	1	2	6	(a,a),(b,b), (c,c),(a,b)
B_1	3	6	18	a,(b,c)	B_g	1	2	6	(a,c),(b,c)
B_2	3	6	18	b,(a,c)	A_u	1	2	6	c
B_3	3	6	18	c,(a,b)	B_u	1	2	6	a,b

c. $P12_1/a1$ (Z=8) site symmetry C_1				
C_{2h}	ν_1	ν_2	$\nu_3+\nu_4$	activity
A_g	2	4	12	(a,a),(b,b), (c,c),(a,c)
B_g	2	4	12	(a,b),(b,c)
A_u	2	4	12	b
B_u	2	4	12	a,c

4. Interpretation of the spectra

In the first part of this section the FIR and Raman spectra presented in section 2 are discussed in terms of the internal modes of the ZCB_n^{2-} ions. A discussion of the external modes will be given in the second part of this section.

4.1. Internal $(ZnCl_{4-n}Br_n)^{2-}$ modes

4.1.1. FIR spectra. Three broad absorption bands are observed in the FIR spectra of the pure compounds, of which two are assigned to the ν_3 and ν_4 internal ZCB_n^{2-} modes (see figure 1). For the pure Cl compound the absorption maxima of these modes are found at approximately $\nu_3 = 275$ cm^{-1} and $\nu_4 = 130$ cm^{-1}, for the Br compound the frequencies are respectively 200 cm^{-1} and 90 cm^{-1}.

The low-frequency absorption band in the spectra is assigned to the external vibrational modes. Due to the weak coupling to the lattice of the internal modes, the tetrahedral symmetry of the ions is almost conserved. Hence, the ν_1 and ν_2 modes are expected to be only weakly absorbing in FIR experiments. In the pure compounds, the ν_2 modes are not observed. In the Cl compound this results from the (near) degeneracy of these modes with the ν_4 modes, whereas in the Br compound the ν_2 modes coincide with the external modes.

The frequencies of the fully symmetric ν_1 modes nearly coincide with those of the ν_3 modes, and are not observed in the spectra. The spectra of the mixed crystals show absorbing bands at the ν_3 frequencies for both pure compounds. These bands result from the ν_3 modes of the pure ions, as well as from the ions with a mixed character. This can be concluded from the valence-bond model (figure 7) and the relative strong intensity of the 200 cm^{-1} band in the $x = 1$, and the 278 cm^{-1} band in the $x = 2.9$ spectra.

The ν_4 absorption band shifts toward lower frequency as x increases, consistent with the valence-bond model. In the spectrum of the $x = 2.9$ compound two absorption dips are observed at 92 cm^{-1} and 109 cm^{-1}. The structure at 92 cm^{-1} is mainly due to the ν_3 modes of the $ZnBr_4^{2-}$ ions. As will be shown later on, the ions with a mixed character present in the $x = 2.9$ crystals are mainly the $ZnClBr_3^{2-}$ ions. We therefore assign the structure at 109 cm^{-1} to the ν_3 internal modes of the $ZnClBr_3^{2-}$ ions.

4.1.2. Raman spectra of the pure compounds. Before we turn to the spectra of the mixed crystals, we will first examine the spectra of the pure compounds, starting with the $x = 4$ compound. In the high-temperature Raman A_g spectrum (figure 2(*a*), upper curve), the four internal modes of the $ZnBr_4^{2-}$ anions are all clearly observed as more or less sharp peaks in the spectrum. In table 4 we have compared the frequencies of these modes with the frequencies measured for the anions in an aqueous solution (Morris *et al* 1963). Since there are only slight differences between these two, we can conclude that the effects of the crystal field on the intra-molecular forces in ZCB_n^{2-} are fairly small. This can also be concluded from the small FWHM (full width at half maximum) of the modes, which indicates only a small splitting of the modes due to the crystal field. In the $x = 4$ Raman B_{1g}, B_{2g} and B_{3g} spectra at 300 K (figure 2(*a*)) we again observe all the internal $ZnBr_4^{2-}$ modes. For the ν_2, ν_3 and ν_4 modes this is expected from the selection rules (table 2). The ν_1 mode, however, should be inactive in B_{1g} and B_{3g} symmetry. The fact that in these cases also a non-zero intensity is found is probably due to the large degree of rotational freedom (Colla 1987) of the $ZnBr_4^{2-}$ tetrahedra around the *a*- and *c*-axis, effectively lowering the site symmetry from C_s to C_1.

Table 4. Comparison of the frequencies of the internal $ZnBr_4^{2-}$ and $ZnCl_4^{2-}$ modes measured by Raman spectroscopy for the crystals with the corresponding frequencies for the ions in an aqueous solution (Morris 1963).

	ν_1	ν_2	ν_3	ν_4
$ZnCl_4^{2-}/H_2O$	275	79	306	104
$[N(CH_3)_4]_2ZnCl_4$	278	116	275*	127
$ZnBr_4^{2-}/H_2O$	172	66	208	88
$[N(CH_3)_4]_2ZnBr_4$	170	56	210	88

* From the FIR data.

In the $x = 4$ low-temperature spectra (figure 2(*b*)), all modes are active in all geometries, consistent with the selection rules (table 3(*c*)). A single ν_1 mode is observed in all geometries and the six different ν_3 and ν_4 modes are better resolved. It is not clear whether the ν_2 modes (2 in each geometry) are resolved due to the coincidence with the external modes.

For the $x = 0$ compound there are some degeneracies which blur the above picture a bit. The ν_2 and ν_4 modes are strongly overlapping and the ν_1 modes are (nearly) degenerate with the ν_3 modes. The latter can be concluded from a comparison of ν_1 modes in the Raman spectra (figure 2(*a*) and 2(*b*), lower curves) with the ν_3 modes in the FIR spectrum (figure 4, lower curve). The comparison of the observed frequencies of the $ZnCl_4^{2-}$ internal modes with those of the ions in an aqueous solution (Morris *et al* 1963) in table 4 shows that in this case the differences are rather large, indicating a non-negligible effect of the crystal field on the intra-molecular forces. This makes the subdivision into external and internal modes in this compound questionable.

In the high-temperature Raman spectra (figure 2(*a*)) again a non-zero intensity is found in the ν_1 region in all geometries. Indeed, part of the intensity in the B_{1g} and B_{3g} spectra can be explained by the activity of the ν_3 mode, as proposed by Meekes *et al* (1988). The large intensity in these geometries indicates, however, that it is also partly due to the activity of the ν_1 modes, again resulting from the large thermal factors of the $ZnCl_4^{2-}$ anions.

In the $x = 0$ low-temperature spectra (figure 2(*b*)) the different modes are as expected active in all geometries. The ν_1 mode is split up into several peaks, reflecting the larger number of formula units in the unit cell in this case (see also table 3(*a*)). It is not clear whether part of the structure in the ν_1 region results from the (weak) activity of the ν_3 modes.

4.1.3. Raman spectra of the mixed compounds. We now turn to the spectra of the mixed crystals. In the Raman spectra (figure 2(*a*) and 2(*b*)) additional peaks appear in the spectra, which are not observed in the spectra of the pure compounds. This is clearest in the region of ν_1, ν_3 modes (150–350 cm^{-1}). These extra modes are due to the presence of mixed $(ZnCl_{4-n}Br_n)^{2-}$ ions in the crystals, indicating that the compounds are true solid solutions, and not just a mixture of the two pure crystals. The peaks in the ν_1, ν_3 region of the A_g Raman spectra at $T = 300$ K (figure 2(*a*)) are fitted to Lorentzian shaped modes. The results of these fits can be found in table 5. The additional modes observed in the ν_1, ν_3 region are assigned to the ν_1 modes (neglecting the ν_3 modes, which generally have a low intensity) of respectively the $ZnCl_3Br^{2-}$ ion (183 cm^{-1}), the $ZnCl_2Br_2^{2-}$ ion (191 cm^{-1}) and the $ZnClBr_3^{2-}$ ion (202 cm^{-1}), based on the qualitative model presented earlier and the results obtained by Delwaulle (1955) for the mixed anions in an aqueous solution. The FWHM of these ν_1 modes increases as the number of Cl atoms in the ion increases (see figure 8), indicating that the ions become more sensitive to the crystal field. This is possibly connected to the large number of phases found for low x values (the anharmonicity of the potential increases as x decreases).

Table 5. Frequencies and relative intensities resulting from fits of the ν_1 modes in the A_g Raman spectra at $T = 300$ K to Lorentzian shaped peaks.

x=0		x=1		x=2		x=2.9		x=4	
ν (cm^{-1})	I_0	ν (cm^{-1})	I_0	ν (cm^{-1})	I_0	ν (cm^{-1})	I_0	ν (cm^{-1})	I_0
				173	13.1	171	43.0	170	93.4
		184	9.7	183	33.0	182	35.9		
		192	28.1	191	17.8	192	4.0		
		202	7.6	202	7.4	205	6.4	210	6.6
278	100	276	54.6	276	28.7	280	10.6		

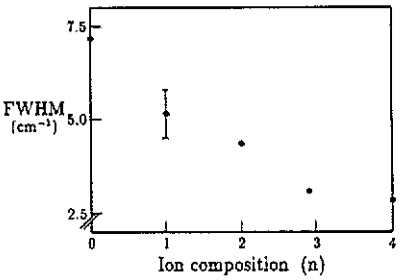

Figure 8. Ion composition (n) dependence for the ZCB_n^{2-} ions of the FWHM of the ν_1 modes in the Raman A_g high-temperature spectra as determined from the Lorentz fits presented in table 5.

Using the intensities listed in table 5, an estimate can be made of the relative concentrations $\rho_n(x)$ of the various ZCB_n^{2-} anions in the different TZCB crystals, which in turn can be used to estimate the value of x. In order to do this, we assume that the intensity of the peaks is only proportional to the concentration of scatterers in the crystal, and therefore one has an equal scattering efficiency for the various ZCB_n^{2-} anions. A problem arises for the $ZnCl_3Br^{2-}$ ion, because the ν_1 mode of this ion is (almost) degenerate with the ν_3 modes of the $ZnBr_4^{2-}$ ion. The influence of the ν_3 modes can be estimated using the intensity ratio $I_0(\nu_3)/I_0(\nu_1)$ of $ZnBr_4^{2-}$ in the spectra of the $x = 4$ compound and the intensity $I_0(\nu_1)$ of $ZnBr_4^{2-}$ in the spectra of the mixed crystals. The estimated values of $\rho_n(x)$ are listed in table 6. This table shows that the $ZnCl_3Br^{2-}$ anion is only present in very low concentrations in the mixed crystals. From the Raman results of Benhmida *et al* (1987) we conclude that the concentration of this ion is only appreciable for very low values of x. It seems that there is a preference to form either the pure anions or mixed ions with more than one Br atom. Table 6 also shows the calculated values x_{calc} of the composition of the crystals. These values lie within 10% of those of the growth solutions, which is a fair agreement in view of the method used to obtain x_{calc}.

Table 6. Relative concentrations $\rho_n(x)$ of the various configurations of the mixed tetrahedra in crystals with different composition (x), calculated from the fitted intensities presented in table 4. From these concentrations the crystal composition x_{calc} has been calculated.

	x				
n	0	1	2	2.9	4
0	100	54.7	28.9	11.0	0
1	0	7.5	6.6	3.5	0
2	0	28.1	18.0	4.1	0
3	0	9.7	33.3	37.0	0
4	0	0	13.2	44.4	100
x_{calc}	0	0.93	1.95	3.00	4

Until now we have been discussing mainly the ν_1 modes of the mixed ions in the Raman high-temperature A_g spectra. The other modes of the mixed ions are not directly observed in the Raman spectra. For the ν_3 modes this is due to their near degeneracy with the ν_1 modes of the tetrahedra. In the FIR spectra we observed two bands in the ν_1,ν_3 region, originating mainly from the ν_3 modes. In our model

(figure 7) the ν_3 frequencies are generally too high. Qualitatively, however, the model predicts two groups of ν_3 modes for the mixed crystals, approximately at the ν_3 frequencies of the pure ions, as is also observed in the FIR spectra.

The ν_2 and ν_4 modes generally overlap with each other, and with the external modes in both the Raman and FIR spectra. In the mixed crystals the ν_2 and ν_4 structure is broadened due to the splitting of the modes, and it shifts towards lower frequency as x increases (see also figure 7). Using the polarized Raman spectra and the selection rules of the ν_1 modes in the *Pnma* phase of the mixed crystals, one can in principle determine whether the site symmetry of the ions is C_s or C_1, and thus obtain some insight in a possible ordering of the substitution of Cl by Br (see section 3). Unfortunately, the large thermal factors of the ions already effectively lowers the site symmetry to C_1 in the pure compounds, as it follows from the ν_1 presence in the B_{1g} and B_{3g} spectra. Therefore the site symmetry of the ions in the mixed crystals is also expected to be C_1, regardless of any ordering in the substitution.

4.2. External modes

In the high-temperature FIR and Raman spectra the external modes are observed as broad structures at low frequencies. The only resolved peak is found at ~ 24 cm^{-1} in the Raman spectra (see figures 2(*a*) and 3). The composition dependence of this mode (see figure 4) suggests that it is a librational mode of the ZCB_n^{2-} ions. This is shown by the dashed curves in figure 4, which give the $k = 0$ frequency dependence of a chain of harmonically coupled rotators with the same moments of inertia as an average ZCB_n^{2-} ion in the corresponding crystal. On the other hand, the pure librational modes of the crystals in the *Pnma* phase are expected to be only Raman active in either A_g and B_{2g} or B_{1g} and B_{3g} geometry, whereas figure 2(*a*) shows that this mode is mainly active in A_g and B_{1g} geometry. Figure 3 shows the temperature dependence of this mode in a $x = 1$ compound. The mode is insensitive to the phase transition to the incommensurate phase at $T_i \approx 291$ K, which is mainly a modulated rotation of the heavy tetrahedra around the *b*-axis. After the transition to the monoclinic $P2_1/n11$ phase at $T_m = 282$ K a hardening of the mode is observed.

Another interesting feature in the high-temperature Raman spectra is the broadening of the Rayleigh wings observed predominantly in the A_g and B_{1g} spectra. The temperature dependence in figure 3(*a*) shows that this broadening decreases as the temperature decreases. Indeed, in the low-temperature spectra (figure 2(*b*)) this broadening has disappeared. This broadening possibly results from quasi elastic scattering from the $N(CH_3)_4^+$ ions due to the large rotational freedom of these ions at higher temperatures (Pauling 1930, Frenkel 1935). At low temperatures this freedom freezes out (Blinc 1979).

5. Conclusions

We have presented polarized Raman spectra and FIR transmission spectra of the solid solution $(N(CH_3)_4)_2ZnCl_{4-x}Br_x$ for $x = 0$, 1, 2, 2.9 and 4 at $T \approx 60$ K and $T \approx 300$ K. In the spectra new modes appear, which are not present in the spectra of the pure Cl and Br crystals. These modes are assigned to the internal modes of the ZCB_n^{2-} ions, in agreement with a simple valence-bond model. The thermal motions of the heavy tetrahedra effectively lower the site symmetry in the high-temperature phase from C_s to C_1. It is therefore not possible to determine from the selection rules whether there

are preferred ion sites for the substitution of Cl by Br. The appearance of all the ν_1 mixed ion modes in the spectra indicate, however, that there are no preferred sites for the substitution.

The most interesting features in the spectra for further investigation are the $\sim 24\ cm^{-1}$ mode of the ZCB_n^{2-} ions, which given its temperature dependence (hardening in the lock-in phase) could be coupled to the soft mode which is responsible for the incommensurate phase. Another interesting feature is the broadening of the Rayleigh wing, possibly caused by quasi-elastic light scattering from the $N(CH_3)_4^+$ ions. This broadening is expected to change discontinuously at the various phase transitions of the crystals. From the temperature and composition dependence of these modes one can gain some more insight into the mechanisms of the phase transitions in this system.

Acknowledgments

We would like to express our thanks to Dr H Meekes and Dr Th Rasing for valuable discussions on the subject, and Professor H van Kempen for his support. This work is part of the research program of the Stichting voor Fundamenteel Onderzoek der Materie (FOM).

References

Arend H, Perret R, Wüest H and Kerkoc P 1986 *J. Cryst. Growth* **74** 321
Benhmida M, Machet R, Jules J-C and Janot B 1987 *Phase Transitions* **9** 111
Blinc R, Burger M, Slak J and Milia F 1979 *Phys. Status Solidi* a **56** K65
Colla E *1987 PhD Thesis* ETH Zürich, Switzerland
Colla E, Gramlich V and Petter W 1987 *Acta Crystallogr.* C **43** 1070
Colla E, Muralt P, Arend H, Perret R, Godefroy R and Dumas C 1984 *Solid State Commun.* **52** 1033
Dam B and Janner A 1986 *Acta Crystallogr.* B **42** 69
Delwaulle M-L 1955 *Bull. Soc. Chem. Fr.* 1294
Edsall John T 1937 *J. Chem. Phys.* **5** 225
Frenkel J 1935 *Acta Phys. Chem.* **3** 23
Janssen T 1986 *Ferroelectrics* **66** 203
Gesi K 1982 *J. Phys. Soc. Japan* **51** 203
Godefroy G 1989 *Phase Transitions* **14** 139
Meekes H, Janner A and Janssen T 1988 *Z. Phys.* B **71** 273
Morris D F C, Short E L and Waters D N 1963 *J. Inorg. Nucl. Chem.* **25** 975
Pauling L 1930 *Phys. Rev.* **36** 430
Sawada S, Shiroishi Y, Yamamoto A, Takashige M and Matsuo M 1978 *Phys. Lett.* **67A** 56
Trouelan P, Lefebvre J and Derollez P 1985 *Acta Crystallogr.* C **41** 846
van Beest B W H, 1986 *Phys. Rev.* B **33** 960
Vogels L J P 1991 *PhD Thesis* KUN Nijmegen, The Netherlands